The 2010 IEEE/RSJ International Conference on
Intelligent Robots and Systems
October 18-22, 2010, Taipei, Taiwan

CPG based Self-adapting Multi-DOF Robotic Arm Control

Woosung Yang, Ji-Hun Bae, Yonghwan Oh, Nak Young Chong, Bum-Jae You and Sang-Rok Oh,
Member, IEEE

Abstract— **Recently, biologically inspired control approaches for robotic systems that involve the use of central pattern generators (CPGs) have been attracting considerable attention owing to the fact that most humans or animals move and walk easily without explicitly controlling their movements. Furthermore, they exhibit natural adaptive motions against unexpected disturbances or environmental changes without considering their kinematic configurations. Inspired by such novel phenomena, this paper endeavors to achieve self-adapting robotic arm motion. For this, biologically inspired CPG based control is proposed. In particular, this approach deals with crucial problems such as motion generation and repeatability of the joints emerged remarkably in most of redundant DOF systems. These problems can be overcome by employing a control based on artificial neural oscillators, virtual force and virtual muscle damping instead of trajectories planning and inverse kinematics. Biologically inspired motions can be attained if the joints of a robotic arm are coupled to neural oscillators and virtual muscles. We experimentally demonstrate self-adaptation motions that that enables a 7-DOF robotic arm to make adaptive changes from the given motion to a compliant motion. In addition, it is verified with real a real robotic arm that human-like movements and motion repeatability are satisfied under kinematic redundancy of joints.**

I. Introduction

It is well known that the walking mechanism in the nervous system by central pattern generators (CPGs) composed of neural oscillators and their network is the fundamental principle for attaining their natural and robust locomotion [1]. Humans or animals exhibit novel natural rhythmic movements such as running, swimming, flying, breathing, etc and continuous arm motions such as turning a steering wheel, rotating a crank, etc. which are dependent upon the interaction between the musculo-skeletal system and the nervous system. Since the musculo-skeletal system is activated like a mechanical spring by means of CPGs and their entrainment property [2]-[5], human behavior is adaptive or robust against unexpected disturbances or environmental changes. Alternate motor commands for the muscles are provided in the CPGs, which enables the musculoskeletal system to deal with environmental perturbations properly afferent feedback of sensory signal [4]–[6].

Relating these previous works, Matsuoka presented a mathematical description of a neural oscillator [2]. He proved that neurons generate a rhythmic patterned output and analyzed the conditions necessary for steady-state oscillations. He also investigated the mutual inhibition networks to control the frequency and pattern [3] but did not include the effect of the feedback on the neural oscillator performance. Employing Matsuoka's neural oscillator model, Taga et al. investigated the sensory signal from the joint angles of a biped robot as feedback signals [4], [5]; they showed that neural oscillators made the robot robust to perturbations through entrainment. Cao et al. [6] proposed the genetic algorithm (GA)-based method to build up desired neural oscillator networks. The CPG based approach was applied later to various locomotion systems [7]–[11] to show that neural oscillators made the robot adaptive to uneven terrains through the entrainment property.

Besides the examples of locomotion, various efforts have been made to strengthen the capability of robots from biological inspiration. Williamson proposed the neuro-mechanical system that was coupled with the neural oscillator for controlling rhythmic arm motions [12]. Arsenio [13] suggested the multiple-input describing function technique to control multivariable systems connected to multiple neural oscillators. However, they only interest in attaining natural adaptive motions by the coupling between the arm joints and neural oscillators. Thus, the correctness of the desired motion was not guaranteed. Specifically, robot arms are required to exhibit complex behaviors or to trace a trajectory for certain type of tasks, where the substantial difficulty of parameter tuning emerges. Yang et al. presented simulation and experiment results in controlling the robotic arm trajectory incorporating neural oscillators for a desired task [14]–[16].

Apart from such the proposed parameter optimization method, we have addressed an intuitive and efficient approach of biologically inspired control [17]. In addition, this work includes the supplemental method to practically enhance the performance with experimental demonstration using the developed 7-DOF robotic arm. Contributions of this approach can be summarized in the following points. 1) In the CPG based control approach, an imposed task on a multi-DOF robotic arm can be attained easily 2) promoting an impressive capability such as self-adapting motions against an unknown disturbance. 3) Also it is needless to solve ill-posedness problems of inverse kinematics and 4) this approach can give an insight into a method of guaranteeing

Manuscript received March 10, 2010;

W. Yang, J.-H. Bae, Y. Oh, B.-J. You and S.-R. Oh are with the Cognitive Robotics Center, Korea Institute of Sci & Tech, Seoul, Korea (e-mail: {wsyang, oyh, ybj and sroh}@kist.re.kr)

J.-H. Bae is with Korea Institute of Industrial Technology, Ansan, Korea (e-mail:joseph@kitech.re.kr)

N. Y. Chong is with the School of Information Science, Japan Advanced Institute of Sci & Tech, Ishikawa, Japan (e-mail: nakyoung@jaist.ac.jp)

motion repeatability of joints in certain regions of the joint space 5) even in redundancy of degrees of freedom (DOFs). For technically accomplishing these objectives, virtual force constraints in terms of Jacobian transpose and virtual muscle damping factors corresponding to the velocity of joints [14] are employed simply to the CPG based controller as desired torques.

In the following section, the proposed biologically inspired control scheme briefly explained. In Section III, stability of the neural oscillator dynamics is described to design the parameters of the neural oscillator. Details of dynamic responses for the verification of the proposed method through experiments are illustrated and discussed in Section IV. Finally, conclusions are drawn in Section V.

II. Biologically Inspired Robotic Systems

A. Conceptual Model

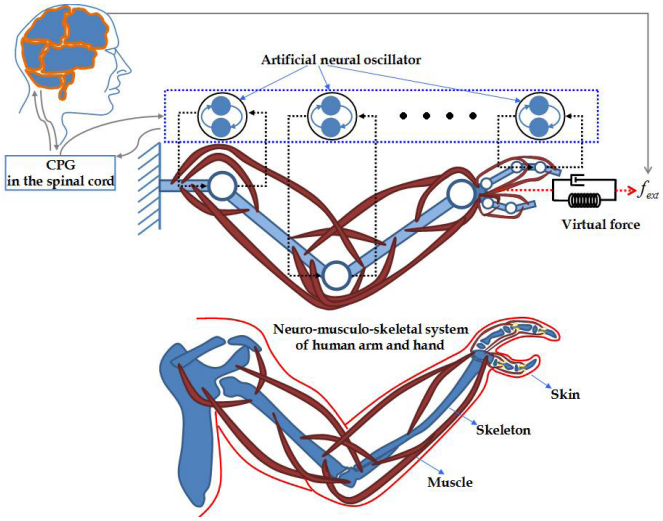

Fig. 1. Conceptual figure of biologically inspired control for a robotic arm/hand

Figure 1 illustrates a schematic model for a robotic arm whose joints are coupled to the neural oscillators. A virtual force leads the coupled robotic arm to a given motion. VFI such as springs and dampers, which are supposed to virtually exist at the target, can be transformed into equivalent torques. This causes the end-effector of a robotic arm to draw according to the target calculating position error. This shows that the ill-posedness of inverse kinematics can be resolved in a natural way without introducing any artificial optimization criterion [18], [19]. However, even with this method, kinematic configurations including redundant joints may not be guaranteed, even though the posture of a robotic arm can only be set within certain boundaries.

From this point of view, it is advantageous if neural oscillators are barely coupled to each joint of a robotic arm. When the oscillators are attached to a robotic arm, they provide proper motor commands that consider the movements of the joints using sensory signals. Since the biologically inspired motions of each joint [17], are attained by the intrinsic entrainment property of the neural oscillator with its network [20] considering each joint direction, the coupled joint can respond intuitively to environmental changes or unknown disturbances by performing an objective motion. In addition, each neural oscillator can be tuned to produce a criterion in terms of the motion limitation of the joints by considering the amplitude of the sensory feedback signal.

B. Artificial Neural Oscillator

Neural motor patterns of vertebrates are obtained from the CPG and modified by sensory signals that detect environmental disturbances. In order to technically accomplish such effects, we used Matsuoka's neural oscillator consisting of two simulated neurons arranged in mutual inhibition, as shown in Fig. 2. If gains are properly tuned, the system exhibits limited cycle behavior. We now propose the control method for dynamic systems that closely interacts with the environment by exploiting the natural dynamics of Matsuoka's oscillator.

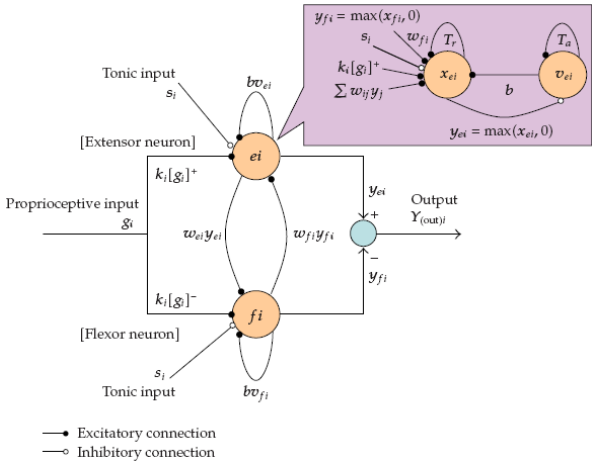

Fig. 2. Schematic diagram of Matsuoka Neural Oscillator

$$
\begin{aligned}
T_r \dot{x}_{ei} + x_{ei} &= -w_{fi} y_{fi} - \sum_{i,j=1}^{n} w_{ij} y_j - b v_{ei} - \sum_{i=1}^{n} k_i [g_i]^+ + s_i \\
T_a \dot{v}_{ei} + v_{ei} &= y_{ei} \\
y_{ei} &= [x_{ei}]^+ = \max(x_{ei}, 0), (i = 1, 2, \cdots, n) \\
T_r \dot{x}_{fi} + x_{fi} &= -w_{ei} y_{ei} - \sum_{i,j=1}^{n} w_{ij} y_j - b v_{fi} - \sum_{i=1}^{n} k_i [g_i]^- + s_i \\
T_a \dot{v}_{fi} + v_{fi} &= y_{fi} \\
y_{fi} &= [x_{fi}]^+ = \max(x_{fi}, 0), (i = 1, 2, \cdots, n)
\end{aligned}
\tag{1}
$$

where x_{ei} and x_{fi} indicate the inner state of the ith neuron for i = 1, 2,…, n, which represents the firing rate. Here, the subscripts e and f denote the extensor and flexor neurons, respectively. $v_{e(f)i}$ represents the degree of adaptation, and b is the adaptation constant or self-inhibition effect of the ith neuron. The output of each neuron $y_{e(f)i}$ is taken as the positive part of x_i, and the output of the oscillator is the difference in the output between the extensor and flexor neurons. w_{ij} is the connecting weight from the jth neuron to the ith neuron: w_{ij} is 0 for $i \neq j$ and 1 for $i = j$. $w_{ij}y_i$ represents the total input from neurons arranged to excite one neuron and inhibit the other. These inputs are scaled by the gain k_i. T_r and T_a are the time constants of the inner state and adaptation effect, respectively, and s_i is an external input with a constant rate. $w_{e(f)i}$ is the

weight of the extensor neuron or flexor neuron, and g_i indicates the sensory input from the coupled system that is scaled by the gain k_i.

C. Coupling mechanical systems to neural oscillators

Figure 3 shows a simple mechanical system coupled to the neural oscillator that is simplified by mimicking neuro-musculo-skeletal model. The desired torque signal to the i-th joint can be given by

$$\tau_i = -k_{oi}(q_i - q_{odi}) - b_i\dot{q}_i, \tag{2}$$

where k_{oi} is the stiffness of the joint, b_i the damping coefficient, q_i the joint angle, and q_{odi} is the output of the neural oscillator that produces neural commands of the i-th joint. The neural oscillator follows the sensory signal from the joints, thus the output of the neural oscillator may change corresponding to the sensory input. This is what is called "entrainment" that can be considered as the tracking of sensory feedback signals so that the mechanical system can exhibit adaptive behavior interacting with the environment.

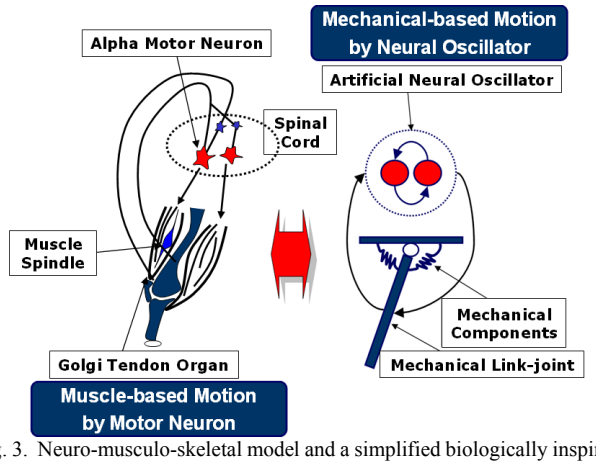

Fig. 3. Neuro-musculo-skeletal model and a simplified biologically inspired mechanical system coupled to the neural oscillator

III. Stability Analysis of the Neural Oscillator

All of the neural models suggested have the common feature of neurons being connected so that one neuron's excitation suppresses another's excitation. Matsuoka developed a more general model with the viewpoint that each neuron is capable of receiving different external stimulus and synaptic weights. However, it is difficult to clearly predict the dynamic responses of the artificial neural oscillator incorporated in Matsuoka's work according to specific conditions, where the oscillation, saturation (or convergence), or divergence occur within a certain range. Also, since Matsuoka neural oscillators have nonlinearities such as max(x, 0) and min(x, 0), as described in (1), it is difficult to analyze their nonlinear behavior. In this section, we discuss the existence of singular points and their stability and use the neural oscillator in time domain analysis to investigate equilibrium states.

Equation (1) of the neural oscillator gives

$$\frac{dx_e}{dt} = g_e(x_e, v_e, x_f, v_f),\ \frac{dv_e}{dt} = f_e(x_e, v_e, x_f, v_f)$$
$$\frac{dx_f}{dt} = g_f(x_e, v_e, x_f, v_f),\ \frac{dv_f}{dt} = f_f(x_e, v_e, x_f, v_f) \tag{3}$$

where g_e, f_e, g_f, and f_f are nonlinear functions of x_e, v_e, x_f, and v_f, respectively. Equation (3) can be rewritten as

$$\begin{Bmatrix} \dot{x}_e \\ \dot{v}_e \\ \dot{x}_f \\ \dot{v}_f \end{Bmatrix} = \begin{bmatrix} a_{11} & a_{12} & a_{13} & a_{14} \\ a_{21} & a_{22} & a_{23} & a_{42} \\ a_{31} & a_{32} & a_{33} & a_{43} \\ a_{41} & a_{42} & a_{43} & a_{44} \end{bmatrix} \begin{Bmatrix} x_e \\ v_e \\ x_f \\ v_f \end{Bmatrix} \tag{4}$$

where

$$a_{11} = \left.\frac{\partial g_e}{\partial x_e}\right|_{(0,0,0,0)} \quad a_{12} = \left.\frac{\partial g_e}{\partial v_e}\right|_{(0,0,0,0)} \quad a_{13} = \left.\frac{\partial g_e}{\partial x_f}\right|_{(0,0,0,0)} \quad a_{14} = \left.\frac{\partial g_e}{\partial v_f}\right|_{(0,0,0,0)}$$
$$a_{21} = \left.\frac{\partial f_e}{\partial x_e}\right|_{(0,0,0,0)} \quad a_{22} = \left.\frac{\partial f_e}{\partial v_e}\right|_{(0,0,0,0)} \quad a_{23} = \left.\frac{\partial f_e}{\partial x_f}\right|_{(0,0,0,0)} \quad a_{24} = \left.\frac{\partial f_e}{\partial v_f}\right|_{(0,0,0,0)}$$
$$a_{31} = \left.\frac{\partial g_f}{\partial x_e}\right|_{(0,0,0,0)} \quad a_{32} = \left.\frac{\partial g_f}{\partial v_e}\right|_{(0,0,0,0)} \quad a_{33} = \left.\frac{\partial g_f}{\partial x_f}\right|_{(0,0,0,0)} \quad a_{34} = \left.\frac{\partial g_f}{\partial v_f}\right|_{(0,0,0,0)}$$
$$a_{41} = \left.\frac{\partial f_f}{\partial x_e}\right|_{(0,0,0,0)} \quad a_{42} = \left.\frac{\partial f_f}{\partial v_e}\right|_{(0,0,0,0)} \quad a_{43} = \left.\frac{\partial f_f}{\partial x_f}\right|_{(0,0,0,0)} \quad a_{44} = \left.\frac{\partial f_f}{\partial v_f}\right|_{(0,0,0,0)}$$

The solutions of (4) should be geometrically similar to those of (3). We assumed the solution of (4) to be in the form

$$\begin{Bmatrix} x_e \\ v_e \\ x_f \\ v_f \end{Bmatrix} = \begin{Bmatrix} X_e \\ V_e \\ X_f \\ V_f \end{Bmatrix} e^{\lambda t} \tag{5}$$

where X_e, V_e, X_f, V_f, and λ are constants. Substituting (5) into (4) leads to the eigenvalue problem

$$\begin{bmatrix} -\frac{1}{T_r} - \lambda & -\frac{b}{T_r} & -\frac{w}{T_r}\delta_f & 0 \\ \frac{1}{T_a}\delta_e & -\frac{1}{T_a} - \lambda & 0 & 0 \\ -\frac{w}{T_r}\delta_e & 0 & -\frac{1}{T_r} - \lambda & -\frac{b}{T_r} \\ 0 & 0 & \frac{1}{T_a}\delta_f & -\frac{1}{T_a} - \lambda \end{bmatrix} \begin{Bmatrix} X_e \\ V_e \\ X_f \\ V_f \end{Bmatrix} = \begin{Bmatrix} 0 \\ 0 \\ 0 \\ 0 \end{Bmatrix} \tag{6}$$

The eigenvalues λ_1, λ_2, λ_3, and λ_4 can be found by solving the characteristic equation of (6) as

$$\lambda_1, \lambda_2, \lambda_3, \lambda_4 = \frac{1}{2}(p \pm \sqrt{p^2 - 4q}) \tag{7}$$

The stability of the neural oscillator is determined by the nature of the eigenvalues of the state matrix. The various combinations of eigenvalues for the matrix of (6) give various characterizations of the equilibrium of the related nonlinear trajectories in the phase plane. The following then holds: 1) if $(p^2 - 4q) < 0$, the motion is oscillatory; 2) if $(p^2 - 4q) > 0$, the motion is aperiodic; 3) if $p > 0$, the system is unstable; and 4) if $p < 0$, the system is stable. Depending on the eigenvalues in (7), singular or equilibrium points can be classified. Hence, investigating the stability on the inner dynamics of the neural oscillator requires the consideration of possible four conditions:

A. Analysis through various cases

1) $x_e > 0$ and $x_f > 0$ ($\delta_e = \delta_f = 1$)

We can obtain the eigenvalues (λ_1, λ_2, λ_3, and λ_4) as described in (7)

$$\lambda_{1,2} = -\frac{1}{2T_rT_a}(T_r + (1-w)T_a) \pm \frac{1}{2T_rT_a}\sqrt{(T_r + (1-w)T_a)^2 - 4(b+1-w)T_rT_a} = \frac{1}{2}\alpha(p_1 \pm \sqrt{(-p_1)^2 - 4q_1}) \tag{8}$$

$$\lambda_{3,4} = -\frac{1}{2T_rT_a}(T_r + (1+w)T_a) \pm \frac{1}{2T_rT_a}\sqrt{(T_r + (1+w)T_a)^2 - 4(b+1+w)T_rT_a} = \frac{1}{2}\alpha(p_2 \pm \sqrt{(-p_2)^2 - 4q_2}) \tag{9}$$

where $p_1 = -(T_r+(1-w)T_a)$, $q_1 = (b+1- w)T_rT_a$, $p_2 = -(T_r+(1+w)T_a)$, $q_2 = (b+1+w)T_rT_a$ and $\alpha = 1/(T_rT_a)$.

- Case 1. The eigenvalues (λ_1, λ_2, λ_3, and λ_4) are real and distinct ($p^2 > 4q$)

In general, the condition for a root of the equation to have positive values in (8) and (9) is

$$T_a^2w^2 \pm 2(T_a^2 - T_rT_a)w + T_a^2 + T_r^2 - 2T_aT_r - 4bT_rT_a > 0 \tag{10}$$

To satisfy (10), the following condition needs to hold:

$$(T_a - T_r)^2 > 4bT_rT_a \tag{11}$$

Under condition (11), the type of motion depends on whether λ_1, λ_2 and λ_3, λ_4 are of the same or opposite sign. $q_1, q_2 > 0$ and $p_1, p_2 < 0$ such that λ_1, λ_2 and λ_3, λ_4 have the same sign. In q_1 and $q_2 > 0$, $(b+1-w)T_rT_a > 0$ and $(b+1+w)T_rT_a > 0$. Then, $b > w-1$ and $b > -w-1$ ($\because T_rT_a > 0$). The equilibrium when $\lambda_1 < \lambda_2 < 0$ and $\lambda_3 < \lambda_4 < 0$ (when λ_1, λ_2 and λ_3, λ_4 are real and negative or p_1 and $p_2 < 0$) then becomes stable since p_1 and $p_2 < 0$, $-(T_r+(1-w)T_a) < 0$, and $-(T_r+(1+w)T_a) < 0$. After rearranging these, $w < T_r/T_a + 1$, $w > -T_r/T_a - 1$. Thus, if $b > \max(-w-1, w-1)$ and $-T_r/T_a-1 > w < T_r/T_a+1$, the neural oscillator is asymptotically stable and converges to a equilibrium point.

On the other hand, if q_1, $q_2 > 0$ and p_1, $p_2 > 0$, the eigenvalues have the same positive sign ($\lambda_1 > \lambda_2 > 0$ and $\lambda_3 > \lambda_4 > 0$), i.e., $b > \max(-w-1, w-1)$, $-(T_r+(1-w)T_a) > 0$, and $-(T_r+(1+w)T_a) > 0$. This condition gives $w < -T_r/T_a - 1$ and $T_r/T_a + 1 > w$. The origin is then at an unstable equilibrium. If λ_1, λ_2 and λ_3, λ_4 are real but of opposite signs (q_1 and $q_2 < 0$ irrespective of the sign of p_1 and p_2), one solution tends to the origin while the other tends to infinity. This is a saddle point with two unstable and two stable manifolds.

Therefore, the stable equilibrium condition can be written as follows:

$$b > \max(-w-1, w-1) \text{ and } -T_r/T_a-1 > w < T_r/T_a+1 \tag{12}$$

The unstable equilibrium condition can be written as:

$$b > \max(-w-1, w-1) \text{ and } w < -T_r/T_a - 1 \text{ and } w > T_r/T_a + 1 \tag{13}$$

Finally, the condition with a saddle point corresponding to unstable equilibrium is written as:

$$b < w-1 \text{ and } b < -w-1 \tag{14}$$

- Case 2. The eigenvaues (λ_1, λ_2, λ_3 and λ_4) are real and equal, respectively. ($p^2 = 4q$)

If p_1 and $p_2 < 0$ ($\lambda_1 < 0$ and $\lambda_2 < 0$), the trajectories are straight lines passing through the origin, and the equilibrium points are stable. Otherwise (p_1 and $p_2 > 0$), the origin is unstable. Thus, the stable condition is

$$-T_r/T_a-1 > w < T_r/T_a+1 \tag{15}$$

In Case 2, the unstable equilibrium condition can be expressed as

$$w < -T_r/T_a - 1 \text{ and } w > T_r/T_a + 1 \tag{16}$$

- Case 3. The eigenvaues (λ_1, λ_2, λ_3 and λ_4) are complex conjugates ($p^2 < 4q$).

In this case, the stability of motion is determined in terms of the criterion illustrated in Case 1. Hence, Case 3 has the same stable and unstable equilibrium conditions.

2) $x_e > 0$ and $x_f < 0$ ($\delta_e = 1$ and $\delta_f = 0$) or $x_e < 0$ and $x_f > 0$ ($\delta_e = 0$ and $\delta_f = 1$)

Both conditions incur similar results. Thus, the eigenvalues are the same if x_e is exchanged for x_f. The eigenvalues of (6) in this condition can be obtained as

$$\lambda_1 = -\frac{1}{T_a}, \quad \lambda_2 = -\frac{1}{T_r} \tag{17}$$

$$\lambda_{3,4} = -\frac{1}{2T_rT_a}(T_r + T_a) \pm \frac{1}{2T_rT_a}\sqrt{(T_r + T_a)^2 - 4T_rT_a(b+1)} = \frac{1}{2}\alpha(p_2 \pm \sqrt{(-p_2)^2 - 4q_2}) \tag{18}$$

where $p_2=-(T_r+T_a)$ and $q_2=T_rT_a(b+1)$ and $\alpha = 1/(T_rT_a)$.

- Case 1. The eigenvaues (λ_3 and λ_4) are real and distinct ($p^2 > 4q$)

In condition (17), λ_1 and λ_2 always have a negative sign since T_r and $T_a > 0$. These eigenvalues are stable. Therefore, by investigating λ_3 and λ_4, the status of the stability can be analyzed. If $q_2 < 0$, then the equilibrium is unstable as a saddle point irrespective of the sign of p since $(b+1)T_rT_a < 0$, $b < -1$. In $q_2 > 0$, the system's stability is stable. By rearranging these conditions, the stable equilibrium condition is as follows:

$$b > -1 \tag{19}$$

while the condition for a saddle point corresponding to unstable equilibrium is given as:

$$b < -1 \tag{20}$$

- Case 2. The eigenvaues (λ_3 and λ_4) are real and equal ($p^2 = 4q$)

This case satisfies the stable condition since $p_2 < 0$ and λ_1, λ_2 always have negative signs.

- Case 3. The eigenvaues (λ_3 and λ_4) are complex conjugates ($p^2 < 4q$).

These are stable and unstable equilibrium conditions identical to Case 1.

3) $x_e < 0$ and $x_f < 0$ ($\delta_e = 0$ and $\delta_f = 0$)

The eigenvalues $\lambda_1, \lambda_2, \lambda_3$, and λ_4 can be obtained by solving the characteristic equation of (6) as

$$\lambda_{1,2} = -\frac{1}{T_r}, \quad \lambda_{3,4} = -\frac{1}{T_a} \tag{21}$$

The equilibrium is always stable since all eigenvalues are real and negative. Therefore, all of the trajectories converge to this equilibrium point, and the system does not oscillate.

B. Discussion through analysis

If the origin of the equation is unstable or has no stable stationary state, then every solution must be oscillatory (not necessarily periodic) due to the boundedness of the solution. The uniqueness and boundedness of the solution for a neural oscillator was proved by Matsuoka [2], [3] assuming that the total input s from the outside of the network is positive and constant with time. If a root of the equation has a positive real part, the stationary solution is unstable. The basic mutual inhibition network consists of a pair of neurons that reciprocally inhibit each other's excitation.

Thus, with the above cases analyzed in subsection A, oscillations in the neural oscillator are generated by the mutual inhibition condition between n neurons with adaptation. Adaptation plays a key role in oscillation generation [3]. If there was no adaptation effect, oscillation would only occur in networks with special structures. In contrast, if a network has strong adaptation, it can easily generate stable oscillation. When the conditions are satisfied, the networks produce and sustain oscillation (not necessarily periodic) for any initial state and any temporary disturbance.

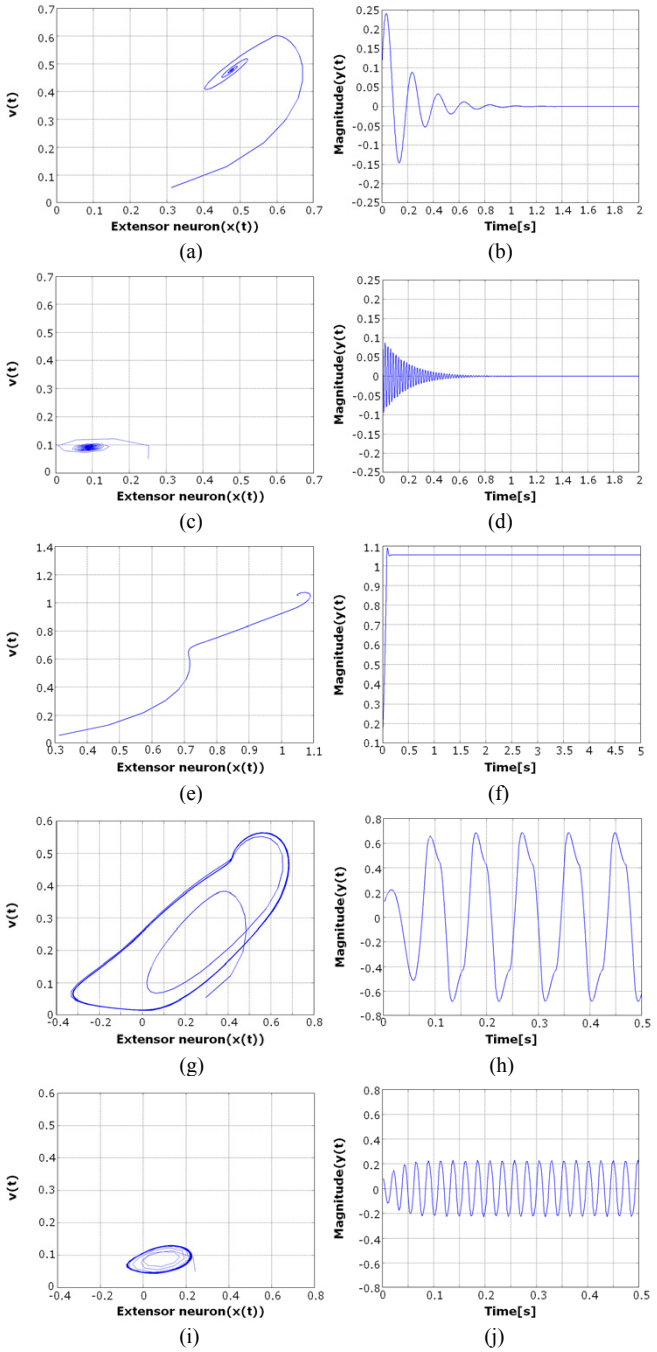

Fig. 4. Plots for analysis of the oscillator dynamics: each row plot is the result when the parameters were sequentially set to w = 10, 10, 10, 15, 100, b = 10, 100, 8.5, 20, 100, and T_r/T_a = 10, 10, 10, 10, 10, respectively: (a), (c), (e), (g) and (i) phase planes of the extensor neuron (b), (d), (f), (h) and (j) the total outputs of the neural oscillator

In conclusion, based on the analysis of the conditions illustrated in subsection A, the conditions for stable oscillation are

$$w > T_r/T_a + 1 \text{ and } b > w - 1 \tag{22}$$

Thus, if the final condition of (22) is satisfied and the synaptic weight w is large enough (though it must be small compared

with b, the network continues oscillating for any large disturbances. Strictly speaking, the system of the differential equations has no stable equilibrium state for the above situation, only strong mutual inhibition.

Based on the above condition (22), various simulations were carried out to verify the theoretical analysis illustrated in subsection A. As shown in Fig. 4, the analysis was verified as achievable. Solutions for the neural oscillator exist within the asymptotically stable region, according to the results shown in Figs. 4(a) to (d). These results were obtained by employing parameters to incur a Case 1 stable equilibrium state in 1). In the results for Figs 4(a) to (d), the frequency and amplitude of the output of the neural oscillator became higher and smaller with increasing b compared to the result shown in Fig. 4(d) due to the adaptation effect. The saddle point condition induced a stable stationary state for the neural oscillator, as shown in Figs. 4(e) and (f). As seen in Figs. 4(g) to (j), which were obtained from condition (22) in subsection A, the oscillation generated in the neural oscillator was verified to be explicitly present in its unstable condition owing to mutual inhibition between the oscillators. In addition, by comparing the result shown in Figs. 4(g) and (h) with that shown in Figs. 4 (i) and (j) appearances such as the frequency and amplitude exposed from these results is similar at significant points with respect to b, which was revealed when Figure 4(a) and (b) was compared with Fig. 4(c) and (d).

IV. Verification with a Real 7-DOF Robotic Arm

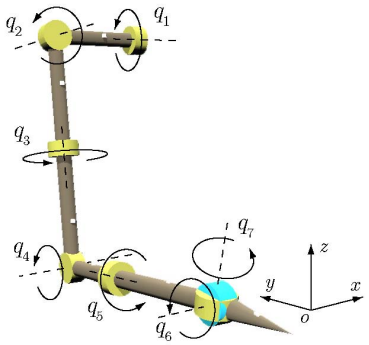

Fig. 5. Geometrical relation of a 7-DOF robotic arm

In this section, we confirm that the neural oscillator and VFI enable the robotic arm to exhibit biologically inspired motion, which enhance its adaptive property sustaining motion stability. Also, in the control scheme, the networks among the oscillators were designed and applied to the proposed approach. The joints $q1$, $q4$ and $q6$ were connected with the excitatory condition of the neural oscillator. There are similar connections to satisfy the condition at the joints $q2$, $q5$ and $q3$, $q7$, respectively. This is helpful in avoiding the ill-posdness and improving adaptability of the proposed control approach. The proposed control approach (see Appendix) is incorporated to a 7-DOF robotic arm developed by the Korea Institute of Science and Technology (KIST), as seen Figs. 1 and 5. Then, we verify whether or not it is possible to generate a desired movement and adapt to unknown disturbances while maintaining the repeatability of each joint motion.

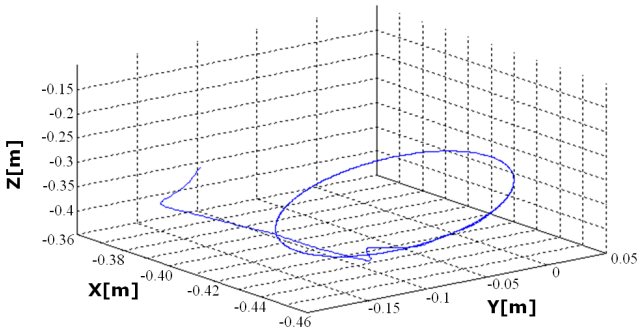

Fig. 6. Trajectory drawn by the end-effector of the 7-DOF robotic arm with respect to the given circular motion in simulation

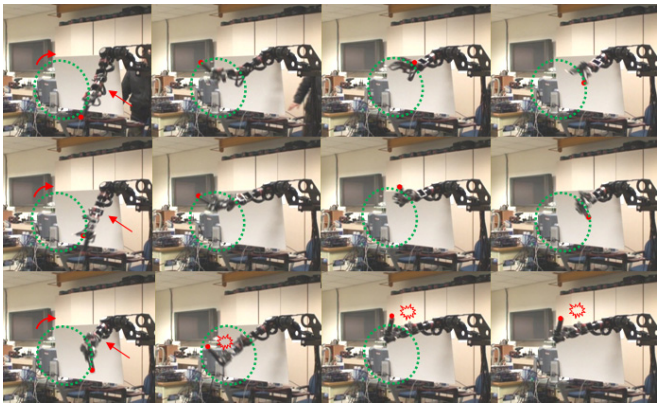

Fig. 7. Snapshots of the experimental results for the 7-DOF robotic arm with respect to the circular motion when sensory feedback of the neural oscillators was turned off.

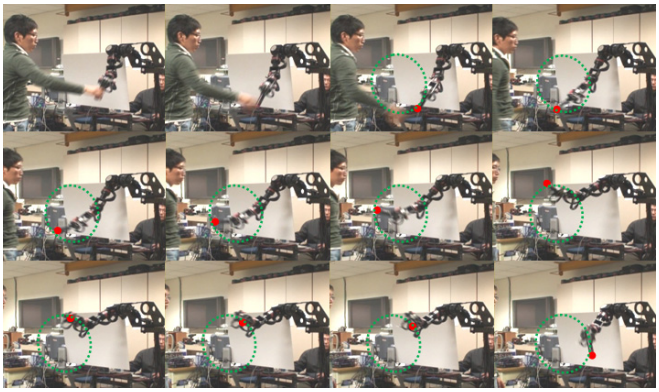

Fig. 8. Snapshots of the experimental results for the 7-DOF robotic arm with respect to the circular motion when sensory feedback of the neural oscillators was turned on

Figure 6 shows the experimental result for the circular motion performed with the real 7-DOF robotic arm. The VFI drives the arm to move according to the given trajectory, and each joint of the robotic arm depends on the outputs generated in the neural oscillator. As expected, the correctness of the arm motion is demonstrated through the result shown in Fig. 6. When controlling a multi-DOF robotic system, if only VFI-based control is considered without using neural oscillators, the repeatability problem for each joint is incurred, as shown in Figs. 7 and 9(a) in contrast with Figs. 8 and 9(b). In Figure 9, the red and blue lines indicate the joint motion

and output of the neural oscillator, respectively. As shown in Fig. 9(b), no alternation of individual joint motions emerged during the circular movement, even in redundant joints, which is in contrast to Fig. 9(a). The joints of the 7-DOF robotic arm were subject to the coupled neural oscillators corresponding to each joint. In Fig. 9(a), the blue line can be ignored because sensory feedback was not fed again. The graph was merely drawn to observe how the neural oscillator was activated. Similar results are shown in Figs. 7 and 8. These figures are the snap shots corresponding to Figs. 9(a) and (b), respectively. Despite the same circular motion being performed in both experiments, the motion in Fig. 7 failed as time went by. In addition, there was an impressive capability for self-adapting motions against unknown disturbance and ill-posedness of inverse kinematics due to the redundant degrees of freedom (DOFs) such as a 7-DOF robotic arm was solved, while the motion repeatability of the joints was sustained.

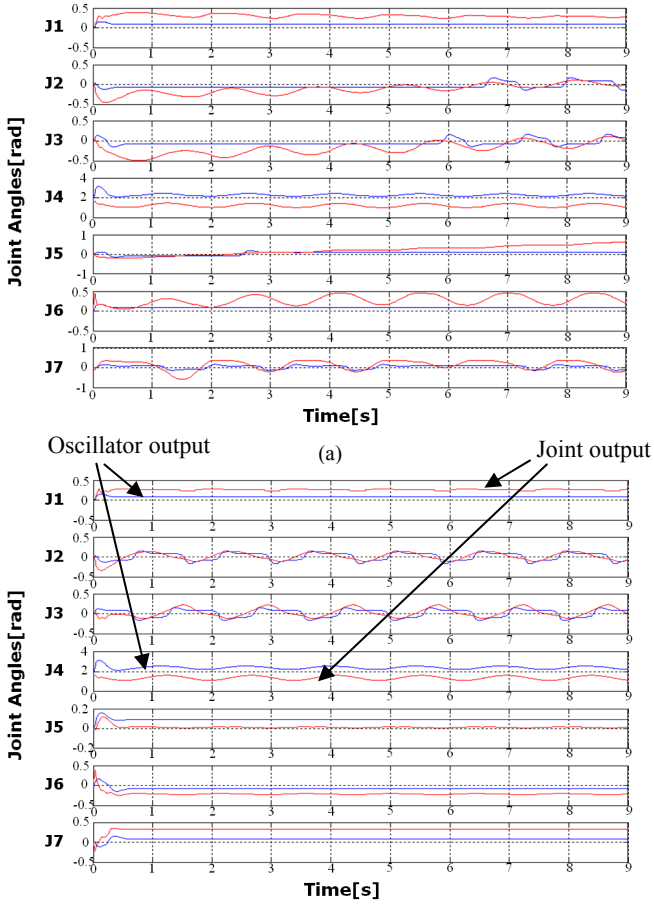

Fig. 9. Individual joint responses acquired during the circular movement in simulation of the 7-DOF robotic arm (a) without coupling to the neural oscillators and (b) with coupling; J1–J7 correspond to each joint in the robotic arm.

Figure 10 illustrates compliant responses that sustained the behaviors carrying out the objectives given to the 7-DOF robotic arm even under unknown disturbances. The red arrow denotes the direction of the applied force. From these results, it is confirmed that the neural oscillator enables the coupled joint to exhibit a biologically inspired motion to enhance adaptive property sustaining motion stability.

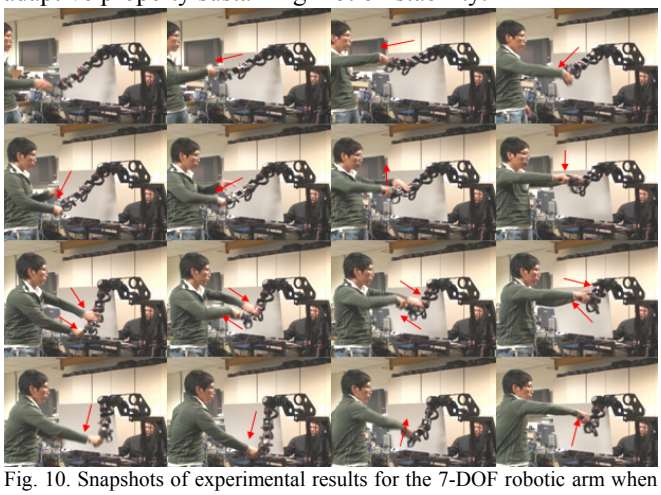

Fig. 10. Snapshots of experimental results for the 7-DOF robotic arm when external disturbances were applied arbitrarily during the circular movement

V. Conclusion

This work mainly addresses how to achieve human-like behavior of multi-DOF robotic arms employing a biologically inspired control scheme. In order to embody the objective of this work, a neural oscillator and VFI (spring and damper) with a muscle damper are incorporated to the proposed control approach. We first focused on robotic behavior to trace a trajectory correctly with virtual components that make it possible to imposed tasks without considering the ill-posedness even in redundant systems. With this, if the joints of multi-DOF robotic systems are coupled to the neural oscillators as CPGs, the biologically inspired system enables robotic behavior to naturally set kinematic configurations with redundancy and guarantee motion repeatability. The effectiveness of such results was exposed in the experiments on the 7-DOF robotic arm. In addition the robotic arm was demonstrated to adapt in response to environmental changes during the experiments keeping the imposed task.

Appendix

In general, dynamics of a robot system with n-th DOFs could be expressed as

$$H(q)\ddot{q}+\left\{\frac{1}{2}\dot{H}(q)+S(q,\dot{q})\right\}\dot{q}+g(q)=u, \tag{23}$$

where, H denotes the $n\times n$ inertia matrix of a robot, the second term in the right hand side of (23) stands for coriolis and centrifugal force, and the third term is the gravity effect. Then a control input for a rhythmic motion of the dynamic system shown in (23) is introduced as follows;

$$u=-C_0\dot{q}-J^T(k\Delta x+\varsigma\sqrt{k}\dot{x})-k_o\Delta q+g(q), \tag{24}$$

where

$$C_0=\mathrm{diag}(c_1,\ c_2,\ \cdots,\ c_n),\ \Delta x=x-x_d,\ \Delta q=q-q_{od}$$

$$c_i = \varsigma_0 \sqrt{k} \sqrt{\sum_{j=1}^{n} \left[H_{ij} \right]},\ (i = 1,\ 2,\ \cdots,\ n)$$

where k and ς_0 is the spring stiffness and damping coefficient, respectively for the virtual components. C_0 is the joint damping. k_o and q_{odi} are the stiffness gain and the output of the neural oscillator that produces rhythmic commands, respectively.

The control inputs as seen in (24) consist of two control schemes. One is based on Virtual spring-damper Hypothesis [18], [19] and the other is determined in terms of the output of the neural oscillator as illustrated in (2). In the control input of (24), the first term describes a joint damping for restraining a certain self-motion which could be occurred in a robot system with redundancy, and the second term means PD control in task space by using of Jacobian transpose, and also a spring and a damper in the sense of physics. Appropriate selection of joint damping factors C_0, stiffness k and damping coefficient ς render the closed-loop system dynamics convergent, that is, x is converged into x_d and both of $\dot{x}$ and $\dot{q}$ are become 0 as time elapses. In general, the neural oscillators coupled to the joints perform the given motion successively interacting with a virtual constraint owing to the entrainment property, if gains of the neural oscillator are properly tuned [15], [16], [19].

Then, closed-loop dynamics with (23) and (24) is expressed as

$$H(q)\ddot{q} + \left\{ \frac{1}{2}\dot{H}(q) + S(q,\dot{q}) + C_0 \right\} \dot{q} + J^T (k\Delta x + \varsigma\sqrt{k}\dot{x}) + k_o \Delta q = 0 \quad (25)$$

The inner product between $\dot{q}$ and the closed-loop dynamics of Eq. (25) yields

$$\dot{q}^T \left[H(q)\ddot{q} + \left\{ \frac{1}{2}\dot{H}(q) + S(q,\dot{q}) + C_0 \right\} \dot{q} + J^T k\Delta x + J^T \varsigma\sqrt{k}\dot{x} + k_o \Delta q \right] = 0 \quad (26)$$

And

$$\frac{d}{dt} E = -\dot{q}^T C_0 \dot{q} - \dot{x}^T \varsigma\sqrt{k}\dot{x} \le 0, \quad (27)$$

where E stands for the total energy

$$E(\dot{q},\ \Delta x,\ \Delta q) = \frac{1}{2}\dot{q}^T H(q)\dot{q} + \frac{k}{2}\left\|\Delta x\right\|^2 + \frac{k_o}{2}\left\|\Delta q\right\|^2 \quad (28)$$

In (28), the first term of the quantity E describes the kinetic energy of the robot system, the second term means an artificial potential energy caused by the error Δx in task space and the error Δq gives rise to an artificial potential energy corresponding to the third term in joint space. As it is well known in robot control, the energy balance relation of (27) shows that the input-output pair $(u,\ \dot{q})$ related to the motion of (26) satisfies passivity.

REFERENCES

[1] Golubltsky, I. Stewart, P.-L. Buono and J. J. Collins, "Symmetry in Locomotor Central Pattern Generators and Animal Gaits," *Nature*, 401: 693-695, (1999).

[2] K. Matsuoka, "Sustained Oscillations Generated by Mutually Inhibiting Neurons with Adaptation," *Biological Cybernetics*, 52:367-376 (1985).

[3] K. Matsuoka, "Mechanisms of Frequency and Pattern Control in the Neural Rhythm Generators," *Biological Cybernetics*, 56:345-353 (1987).

[4] G. Taga, "A model of the Neuro-musculo-skeletal System for Human Locomotion. I. Emergence of basic gait," *Biological Cybernetics*, 73:97-111 (1995).

[5] G. Taga, "A model of the Neuro-musculo-skeletal System for Human Locomotion. II. Real-time adaptability under various constraints," *Biological Cybernetics*, 73:113-121 (1995).

[6] S. Rossignol, "Neural Control of Stereotypic Limb Movement," *New York: Oxford University Press*, Chap. 12: 173-216, (1996).

[7] S. Miyakoshi, G. Taga, Y. Kuniyoshi, and A. Nagakubo, "Three-dimensional Bipedal Stepping Motion Using Neural Oscillators-Towards Humanoid Motion in the Real World," *Proc. IEEE/RSJ Int. Conf. on Intelligent Robots and Systems*, 84-89 (1998).

[8] Y. Fukuoka, H. Kimura and A. H. Cohen, "Adaptive Dynamic Walking of a Quadruped Robot on Irregular Terrain Based on Biological Concepts," *The Int. Journal of Robotics Research*, 22:187-202 (2003).

[9] G. Endo, J. Nakanishi, J. Morimoto and G. Cheng, "Experimental Studies of a Neural Oscillator for Biped Locomotion with QRIO," *Proc. IEEE/RSJ Int. Conf. on Intelligent Robots and Systems*, 598-604 (2005).

[10] W. Yang, N. Y. Chong, C. Kim and B. J. You, "Self-adapting Humanoid Locomotion Using a Neural Oscillator Network," *Proc. IEEE/RSJ Int. Conf. on Intelligent Robots and Systems*, 309-316 (2007).

[11] W. Yang, N. Y. Chong, S. Ra, C. Kim and B. J. Y, "Self-stabilizing Bipedal Locomotion Employing Neural Oscillators," *Proc. IEEE-RAS Int. Conf. on Humanoid Robots*, 8-15 (2008).

[12] M. M. Williamson, "Rhythmic Robot Arm Control Using Oscillators," *Proc. IEEE/RSJ Int. Conf. on Intelligent Robots and Systems*, 77-83 (1998).

[13] A. M. Arsenio, "Tuning of neural oscillators for the design of rhythmic motions," *Proc. IEEE Int. Conf. on Robotics and Automation*, 1888-1893 (2000).

[14] W. Yang, N. Y. Chong, C. Kim and B. J. You, "Optimizing Neural Oscillator for Rhythmic Movement Control," *Proc. IEEE Int. Symp. on Robot and Human Interactive Communication*, 807-814 (2007).

[15] W. Yang, N. Y. Chong, Jaesung Kwon and B. J. You, "Self-sustaining Rhythmic Arm Motions Using Neural Oscillators," *Proc. IEEE/RSJ Int. Conf. on Intelligent Robots and Systems*, 3585-3590 (2008).

[16] W. Yang, N. Y. Chong, C. Kim and B. J. You, "Entrainment-enhanced Neural Oscillator for Rhythmic Motion Control," *Journal of Intelligent Service Robotics*, 6:.303-311 (2008).

[17] W. Yang, J.-H. Bae, J. Kwon, N. Y. Chong, Y. Oh and B. J. You, "Self-adapting Robot Arm Movement Employing Neural Oscillators," *Proc. IEEE/RSJ Int. Conf. on Intelligent Robots and Systems*, 2235-2242 (2009).

[18] S. Arimoto, M. Sekimoto, H. Hashiguchi and R. Ozawa, "Natural Resolution of ill-Posedness of Inverse Kinematics for Redundant Robots: A Challenge to Bernstein's Degrees-of Freedom Problem," *Advanced Robotics*, 19: 401-434 (2005).

[19] S. Arimoto, M. Sekimoto, J.-H. Bae and H. Hashiguchi, "Three-dimensional Multi-Joint Reaching under Redundancy of DOFs," *Proc. IEEE/RSJ Int. Conf. on Intelligent Robots and Systems*, 1898-1904 (2005).

[20] W. Yang, N. Y. Chong, C. Kim and B. J. You, "Self-adapting Humanoid Locomotion Using a Neural Oscillator Network," *Proc. IEEE/RSJ Int. Conf. on Intelligent Robots and Systems*, pp. 309-316, (2007).